Cruise Report
RV Hercules
Valletta-Valletta, 1.-10.10.2018
MARCAN Project

Contents

1. Participants

Name	Role	Institution
Prof. Aaron Micallef	Chief Scientist	University of Malta
Prof. Christian Berndt	Co-chief Scientist	GEOMAR Germany
Dr. Janine Berndt	Scientist	-
Dr. Marion Jegen	Co-chief Scientist	GEOMAR Germany
Dr. Katrin Schwalenberg	Scientist	BGR, Germany
Martin Wollatz-Vogt	Technician	GEOMAR, Germany
Dr. Amir Haroon	Scientist	GEOMAR, Germany
Dr. Xavier Garcia	Scientist	CSIC, Spain
Zahra Faghih	Student	GEOMAR Germany
Dr. Daniele Spatola	Scientist	University of Malta
Dr. Tamara Worzewski	Journalist	Germany
Johannes Zerbst	Camera person	Germany

2. Background

Coastal regions are the most densely populated areas in the world with an average population density nearly 3 times higher than the global average. Freshwater resources in coastal states and island nations are therefore under enormous stress, and their quantities and qualities are rapidly deteriorating. This problem is exacerbated by population growth, pollution, climate change and political conflicts. Problems are especially felt in arid areas, such as Malta, where groundwater is the only source of freshwater and the periods of highest demand (e.g., agricultural and tourist seasons) coincide with the periods of lowest recharge from precipitation. By comparison, Cape Town, South Africa is the first major city in the modern era to face the threat of running out of drinking water, and other large cities like Jakarta, and Beijing are likely to follow suit.

Offshore aquifers (OAs) have been proposed as an alternative source of freshwater to cover demand by domestic, agricultural and tourist industries in coastal regions. During the Last Glacial Maximum (19-22,000 years ago), modern shelf areas were sub-aerially exposed, leading to the development of extensive water tables recharged by atmospheric precipitation (meteoric water), rivers, lakes and, in some areas, glacial melt water. In view of the fact that sea level has been much lower than today for 80% of the Quaternary period (last 2.6 million years), and that meteoric groundwater systems migrate landwards more slowly than rising sea levels, remnants of meteoric groundwater occur extensively offshore.

Two types of OAs can be distinguished (Figure 1). The first type (active) entails a present-day, permeable connection of the OA with a terrestrial aquifer recharged by meteoric water. Such aquifers tend to be wedge-shaped, becoming thinner and more saline with increasing distance from the coast. However, onshore hydraulic heads are sometimes too low to drive water offshore or a hydraulic connection between offshore and onshore aquifers may be absent. In such cases, offshore groundwater systems are associated with paleo-groundwater (fossil) systems that have been emplaced by meteoric recharge during lowered sea level periods and that are no longer recharged. Recent studies have estimated the volume of OAs to range between ~ 3×10^5 km^3 and 4.5×10^6 km^3, with a more robust estimate of 5×10^5 km^3. The latter is two orders of magnitude greater than what has been extracted globally from continental

aquifers since 1900. Since submarine groundwater can be exploited using conventional technology from the oil and gas industry and onshore groundwater exploitation, and because the costs seem to be economically competitive with desalination, OAs have the potential to become an important resource that can relieve water scarcity and mitigate the adverse effects of groundwater depletion (e.g. land subsidence, saltwater intrusion) in densely populated coastal regions. The characteristics of offshore groundwater systems remain poorly constrained, and there are many first-order questions, related to aquifer geometry and distribution, that need to be addressed. Conventional offshore groundwater aquifer and submarine groundwater discharge (SGD) methods rely on point-source data from boreholes, seepage meters, and chemical radionuclide tracer techniques that cannot provide continuous information of the groundwater system. Additionally, most measurements and research efforts have focused on the nearshore zone (up to several km from the shoreline), mainly because of accessibility, the presence of observable discharge at low tides, and its direct association with the unconfined surficial aquifer and topographically driven flow.

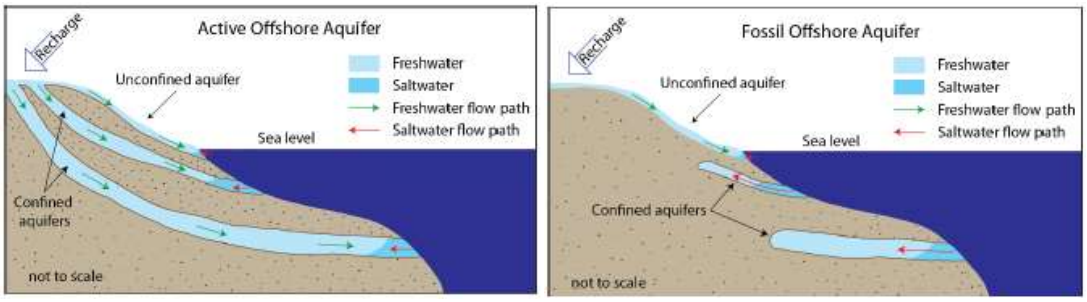

Figure 1: *Cartoon depicting the differences between active (connected) and fossil (disconnected) offshore aquifers. The modern day active aquifers are recharged by precipitation (green arrows). Fossil aquifers are no longer fed by meteoric water and are subject to saltwater intrusion (red arrows).*

Malta is representative for a large part of the carbonate Mediterranean coastline, and is also one of the ten poorest countries globally in terms of water resources per inhabitant. Terrestrial hydrogeological investigations on Malta define two aquifers: a perched aquifer in the Upper Coralline Limestone (high porosity) and a mean sea-level Ghyben-Herzberg freshwater lens in the Lower Coralline Limestone with lower porosity, separated by an impermeable “Blue Clay” layer.

3. Objectives

The overarching goal of the cruise was to detect and characterise sub-seafloor evidence of offshore groundwater.

The study area is located along the east coast of Malta, where all the relevant formations hosting the aquifers occur and where the highest probability that an impermeable layer (Blue Clay) may extend offshore providing a seal for a potential offshore aquifer. The study area exhibits the widest and most gently sloping part of the Maltese continental shelf and bedrock/outcrop scarcity makes it the most suitable location for geophysical investigations. Further indicators of the potential OA occurrence are a series of box canyons that are located upslope of a limestone cliff and observations of flares in sub-bottom profiles. While the OA indications are indirect within the Malta regions, extensive groundwater seeps documenting the presence of OA have been located offshore in very similar geological settings, particularly offshore Sicily and the Levant.

4. Methods

4.1 Marine controlled-source electromagnetics (CSEM)

4.1.1 Background

Marine controlled-source electromagnetics (CSEM) is a geophysical exploration method used to derive the electrical properties, i.e. resistivity, of the seafloor. Electrical conduction in seafloor sediments occurs through ions in pore fluids, and therefore the conductivity (1/resistivity) of seafloor sediments depends mainly on the sediment porosity, pore space connectivity and the conductivity (ion content) of the pore fluid. An important source for ions is the amount of salt in the pore fluid; therefore, the conductivity of the pore fluid depends strongly on its salinity. Figure 2 shows the relationship between salinity and pore fluid conductivity at different temperatures. The relationship between the bulk resistivity of the sediment, porosity and pore fluid resistivity may be described by the experimentally derived Archie's Law, which holds for most sediments with little clay content:

$$\rho_{bulk} = a\, \phi^{-m}\, S^{-n}\, \rho_{fluid}$$

Where $\boldsymbol{\rho}_{bulk}$ and $\boldsymbol{\rho}_{fluid}$ is the resistivity of the seafloor and pore fluid respectively, $\boldsymbol{\phi}$ is the porosity, *S* the pore fluid saturation, and *a, m* and *n* are constants, which range between 0.5-1.5, 1.8-2.4 and ~2, respectively in marine sediments.

Typical seawater resistivity varies between 0.3 to 0.33 Ohm m, depending on the seawater salinity and shallow marine sediments typically have a bulk resistivity of around 1 Ohm m. Fresh water resistivity ranges between 1 and 10 Ohm m, thus the bulk resistivity increases by a factor of 3 to 30 for fresh water saturated sediments.

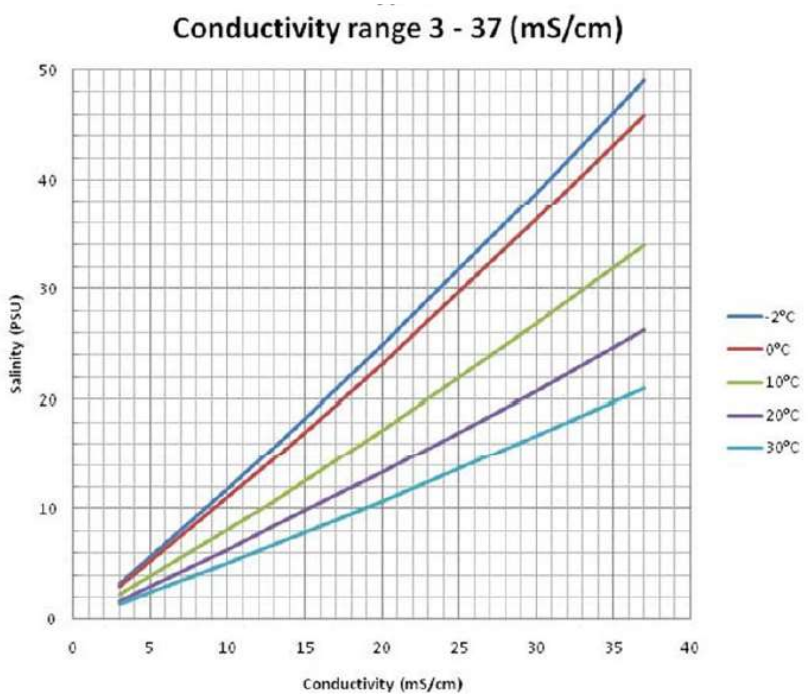

Figure 2: *Pore fluid conductivity for different salinity values and temperatures.*

Bulk electrical resistivity of marine sediments can be derived from CSEM data. For this, an electromagnetic wave is generated through a seafloor transmitter, which subsequently diffuses outward (Figure 3). The wave's diffusion speed and amplitude damping is a function of seawater and seafloor resistivity. The speed increases with increasing resistivity while amplitude damping decreases with increasing resistivity. Through monitoring the shape of the electromagnetic wave at different offsets, a resistivity model may be derived via inversion. The inversion is a statistical search process, which identifies resistivity models with responses that fit well with the instrumented responses. Short offset data and early time signals are most sensitive to shallow structures, while long offset data and late time signals contain information about the deeper structures (penetration depth is about 1/3 of the offset).

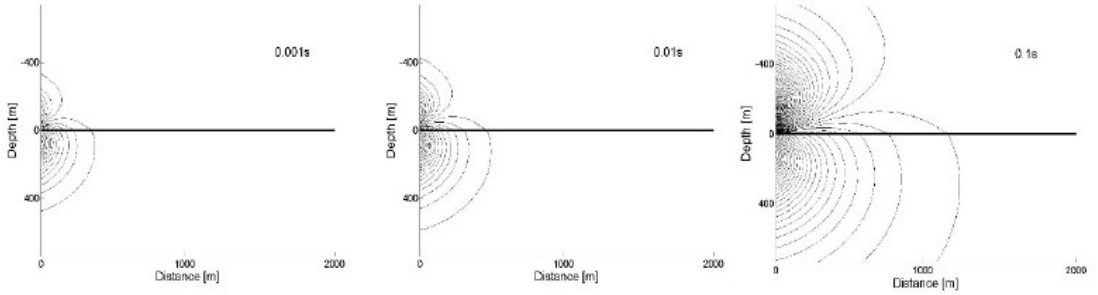

Figure 3: *Snapshots of the propagation of an electrical dipole field generated at the seafloor (black line) at 0.001, 0.01 and 1 sec after current switch on in transmitter dipole. The sea-layer and seafloor are assumed to be infinitely thick with a resistivity of 0.3 Ohm and 1 Ohm, respectively.*

Figure 3 shows snap shots of the propagation of an electric dipole wave as created by the transmitter used in the experiment. The response as a function of time for a receiver 100 m away from the transmitter is shown in Figure 4 for seawater/ sub-seafloor conductivity of (σ_1/σ_2) contrasts ranging between 1 and 30. The response changes significantly for different conductivity contrasts. For high conductivity contrasts (e.g. low conductivity seafloor and a high conductivity sea layer), the early arrival of the seafloor wave can be easily distinguished from the later time arrival of the sub-surface layer wave. If there is not a strong contrast, the waves do not distinctly separate in time yet the transient is altered in amplitude.

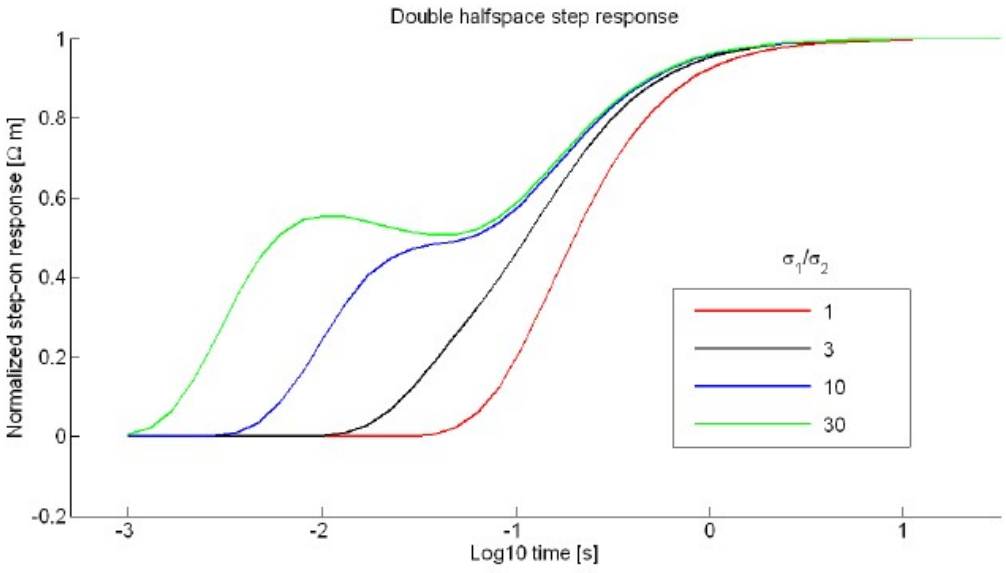

Figure 4: *Electric seafloor dipole-dipole response for a switch on transmitter current waveform at 100*

m transmitter-receiver offset. Response is shown for different conductivity contrasts between the seafloor (σ_2) and a subsurface layer (σ_1) (from R.N. Edwards).

Where CSEM measurements are performed in relatively shallow waters compared to the transmitter-receiver distance, the so-called airwave can have a significant effect on the signal. For shallow oceans, a fast or even the fastest path to the receiver may actually be through the sea layer into the very resistive air and back through the sea-layer to the seafloor receiver. This airwave may mask other arrivals of waves through seafloor resistors, thus making a visual qualitative interpretation of the data more difficult.

4.1.2 Instrumentation

The seafloor-towed CSEM System HYDRA developed by BGR is a modular electric dipole-dipole system consisting of a 100-m-long electrical transmitting dipole and 4 electrical receiving units (Figure 5). Transmitting dipole and receiving units are connected with rope at offsets from 150 m to about 650 m. A stainless steel tow-body termed the "pig" is attached to the front end of the seafloor array. It has the function of a weight to keep the array on the seafloor and serves as an instrument platform. It hosts the GEOMAR transmitter system that consists of three pressure cylinders containing the electronics capable of transmitting currents up to 50 A. The pig also contains a CTD sensor and an acoustic transponder for navigation purposes. A mobile winch with 700m of opto-electrical cable is used to tow the array behind the ship.

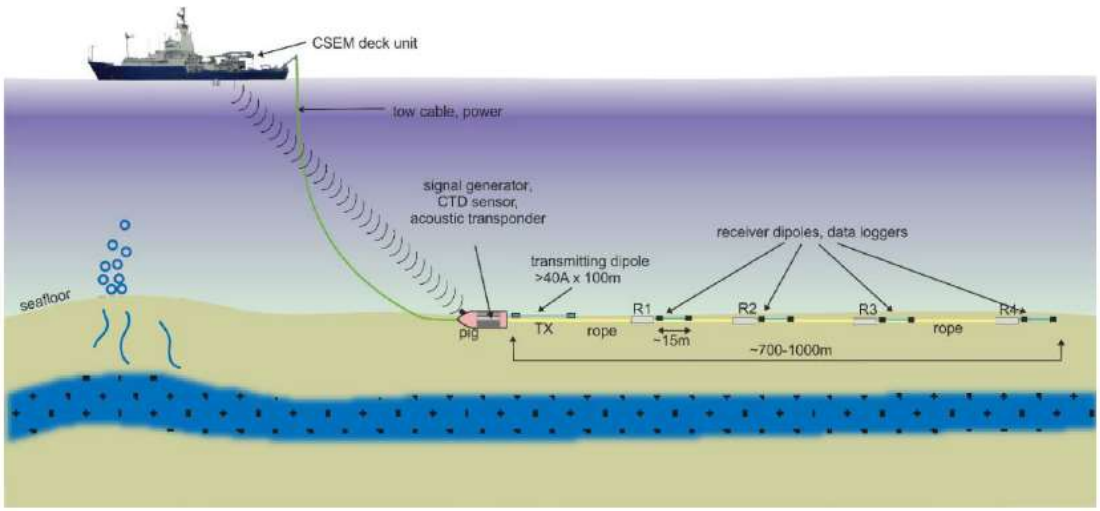

Figure 5: *Set-up of the towed electric dipole-dipole system used in this cruise.*

Winch and block

The CSEM system is deployed and towed directly from its own self-contained electro-hydraulic tow winch that holds 700 m of 22-mm-diameter electro-optical cable with a peak tension load of 16 tons (Figure 6) (DT Marine Tow Winch Model 1020EHLWRS). For the cruise, the winch was welded to the aft deck at a distance of approximately 10 m from the stern. A block fitting the 22 mm cables was installed next to the block usually used for ROV deployment. In front of the winch, a smaller-scale Joko winch has been installed to facilitate the deployment and recovery of the receiver string.

Figure 6: *Winch (blue with green cable) and winch block (green) on A-frame. The winch was welded onto the deck.*

Depressor (Pig)

The pig (Figure 7) is a stainless steel casing with a weight of 450 kg in air constituting the front end of the electric dipole-dipole seafloor array. For the MARCAN experiment the pig hosts the pressure vessels with GEOMAR transmitter electronics, a CTD sensor and an acoustic transponder provided by the RV Hercules. The pig was deployed with a crane through the A-frame onto the swimming platform at the stern of the ship. The weight was then picked up by the winch cable and the pig was lowered into the water. Usual readings on the tensiometer on the DT winch were 300 to 400 N. Timing on the transmitter is supplied by a chip-scale atomic clock.

Figure 7: *Stainless steel depressor containing GEOMAR transmitter (3 pressure housings with lead batteries, H-bridges and electronics). CTD sensor is mounted within pig at the back end on one of the railings, transponder on white POM holder above the pig's nose.*

Transmitter

The GEOMAR transmitter has been developed in-house and consists of H-Bridges, three DC-DC converters and a data logger/controller with a modem. Power to the transmitter is supplied by rechargeable lead gel buffer batteries. The transmitter supplies up to 50 A current in a full or half duty cycle through copper current electrodes (Figure 8). The distance of the copper current electrodes for this experiment was chosen to be 100 m and the period of the duty cycle was chosen to be 4 or 8 seconds. The transmitter is linked to the ship by the DT 22 mm electro-optical winch cable, which serves as a power lead to the transmitter and also as a modem line to communicate real-time with the transmitter. The lead gel batteries serve as a power buffers to the transmitter and are recharged during transmission pauses. The transmitter is synced to a very stable, chip-scale atomic clock. Maximum drifts observed over 24 hours were 0.2 ms. For safety reasons, the transmitter is switched on after it has been launched, usually at a water depth of approximately 20 m, and is switched off before it reaches the water surface at recovery.

Figure 8: *Transmitter current electrode.*

Hydra Receiver

The HYDRA receivers are battery-powered low-noise data loggers recording the receiver dipole voltages with 22 bit ADC at a sampling rate of 10 kHz. The receiver electronics have been developed and built by MAGSON GmbH Berlin (Figure 9). A precise time signal is provided by chip-scale atomic clocks, which are synchronised to GPS time prior to each deployment.

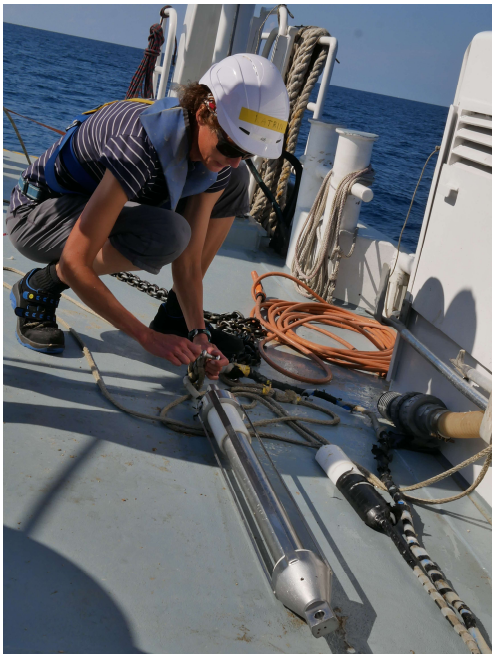

Figure 9: *Hydra receivers from MAGNSON. The instruments used on the cruise were on loan from the BGR, Hannover.*

CTD

We used a Microcat CTD from Seabird (model SBE 37-SM) capable of measuring conductivity, temperature and depth autonomously. The system was attached to the back of the pig onto one of the internal rails to protect it from being damaged during deployment or recovery. The system was set to UTC time using a model cable and the sampling frequency was chosen as 0.1 Hz for all deployments. The position of the CTD can be determined via the time line of the transponder position on the pig. The acquired CTD data was converted to salinity, velocity, conductivity, density, temperature values.

4.1.3 Data Acquisition

The system is deployed by letting the receiver streamer, consisting of 2 or 3 electrical receiver dipoles separated by ropes of predefined length and some weights, into the water. The receiver array is assembled on deck during the deployment. After synchronisation of the receiver logger in the laboratory, it is carried onto the deck and mounted to a holder and electrically connected to an electrical dipole consisting of two Silvion electrodes spaced 10 to 20 m apart. The first item in the water is a weight consisting of metal chains, followed by the furthest receiver dipole of the array. A rope is then connected to the holder and unwound from the Joko winch (Figure 10, left). During this process, the ship is moving forward with about 0.5 to 1 kn to ensure that the dipole and rope are stretched out on the seafloor. Another receiver dipole is then assembled, connected to the array and the next rope length is unspooled from the Yoko winch. The procedure is repeated for the remaining receivers and the transmitter dipole with the current electrodes. Lastly, the transmitter dipole is mechanically fastened to the pig and electrical connections to the transmitter dipole are established. The transmitter is then synched to GPS time.

Figure 10: Joko winch carrying the rope lengths for receiver array (left), DT Winch with 22 mm cable (middle) and controlling station in laboratory (right).

The deployment of the pig was challenging since part of the A-frame was occupied by a ROV head. We therefore had to use the starboard crane to lift the pig through the A-frame onto the swimming platform at the stern of the ship. At this point, the weight was picked up with the DT winch cable (Figure 10, middle). After a successful test at 20 m water depth, the system was further lowered onto the seafloor, maintaining a ship's speed of about 0.5 to 1 kn. The entire deployment procedure on board the RV Hercules took about 1.5 hours, thus resulting into a lead length into the profile of about 1.5 nm. Touch down of the pig onto the seafloor caused the tension on the cable to drop from 400 N to about 200 N or less. At this point an additional 100 m of cable was paid out in order to ensure that the entire array remained on the seafloor during towing. The position of the transmitter is identified through the pig mounted transponder and supplied by the ship. The navigation string was displayed via Fledermaus software on a screen in the lab and also recorded as log files. The log files are later used to establish time-position arrays for the transponder position, allowing one to determine the exact position of the array from the times on the transmitter and receiver. A separate laptop in the lab was used for a modem connection to the transmitter and controls (amplitude and duty cycle period) and monitors the transmitter functioning (Figure 10 right).

The transmitter wave used was a rectangular half duty cycle with an amplitude of 20 A and a period of initially 4 seconds, which was later increased to 8 seconds. The transmission and recording at the receiver was continuous. To reduce motion noise and to increase signal to noise level, we stopped the array for a few minutes along a sequence of waypoints along each profile. All together 93 waypoints were acquired along the 9 profiles. A sample data set is shown at way point 1 on profile 9 in Figure 11.

The receiver and transmitter settings for all deployments are summarised in Table 1, dates and details for each profile are listed in Table 2. A diagram in Figure 12 summarises the geometric array parameters for each deployment. Figure 13 shows the spatial coverage of the CSEM survey.

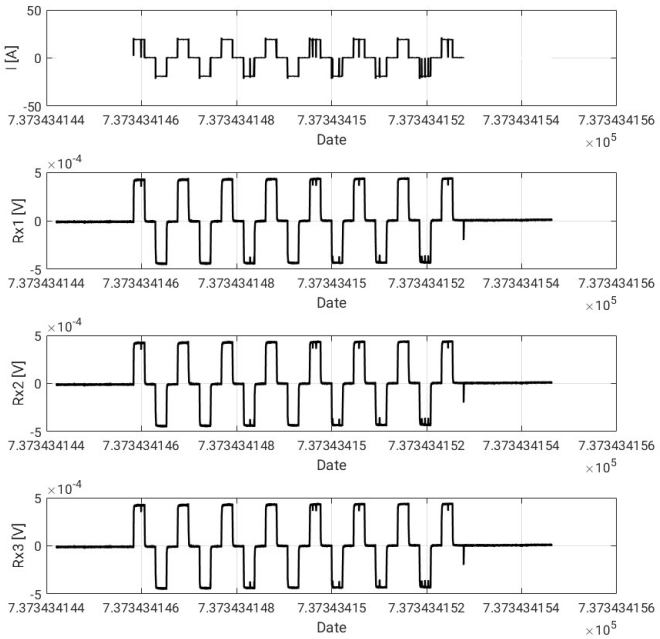

Figure 11: *Sample transmitter data (top panel) and received Earth's response at three different receivers of the array. The data was acquired at waypoint 1 of Profile 9.*

Table 1: *Details on receiver and transmitter settings for the different deployments.*

Date	Deployment	TX-RX1 offset (m)	TX-RX2 offset (m)	TX-RX3 offset (m)	Receiver Dipole length (m)	Hydra
04.10.18		149.11	474.7	-	R1: 10.37 R2: 14.54	R1: Hydra 107, gain 0 R2: Hydra 109, gain 1
05.10.18 (repeat the 04.10.18)	Profile 9	149.11	474.7	-	R1: 10.37 R2: 14.54	R1: Hydra 107, gain 0 R2: Hydra 109, gain 1
06.10.18	Profile 6 Profile 5	149.11	272.54	500.08	R1: 10.37 R2: 14.54 R3: 20	R1: Hydra 107, gain 0 R2: Hydra 108, gain 1 R3: Hydra 110, gain 2
07.10.18	Profile 2	149.025	272.52	500.06	R1: 10.25 R2: 14.54 R3: 20	R1: Hydra 107, gain 0 R2: Hydra 108, gain 1 R3: Hydra 110, gain 2
08.10.18	Profile 5	149.025	272.49	500.06	R1: 10.25 R2: 14.54 R3: 20	R1: Hydra 107, gain 0 R2: Hydra 108, gain 1 R3: Hydra 110, gain 2
09.10.18	Profile 8	149.025	272.52	500.06	R1: 10.25 R2: 14.54 R3: 20	R1: Hydra 107, gain 0 R2: Hydra 108, gain 1 R3: Hydra 110, gain 2
10.10.18	Profile 9	149.025	272.49	500.06	R1: 10.25 R2: 14.54 R3: 20	R1: Hydra 107, gain 0 R2: Hydra 108, gain 1 R3: Hydra 110, gain 2

Table 2: *Details on data acquisition for the different profiles.*

Start Date (UTC)	Deployment Information	Note
04.10.2018 Profile 9	Start: 16:40 End: 18:10 Duration: 1h 30min	- This deployment was carried out to test the equipment. - RX clocks synced but not to GPS time prompt. - TX 4 s period
05.10.2018 Profile 9	Start: 15:20 End: 17:30 Duration: 2h 10min Waypoints: 10	- Last deployment was repeated (Profile 9). - Transmitted failure at 17:30, survey stopped. - RX clocks synced but not to GPS time prompt. - 17:18 reboot of transmitter, Ethernet on laptop broken.
06.10.2018 Profile 6 Profile 5	Start: 11:20 (PIG in the water) End: 14:30 Duration: 3h 10min Waypoints: 11 Start: 17:00 End: 18:00 Duration: 1h Waypoints: 4	- R1 dipole was broken. - TX 8 s period
07.10.2018 Profile 2	Start: 13:00 End: 16:15 Duration: 3h 15min Waypoints: 16	- R1 dipole was repaired, the offsets were changed slightly. - TX 4 s period
08.10.2018 Profile 5	Start: 10:40 End: 15:55 Duration: 5h 15min Waypoints: 24	- 300 m offsets between waypoints. - 100 m offset between WP6 and WP7. - 150 m offset between WP7 and WP8, WP8 and WP9, WP9 and WP10, WP10 and WP11.
09.10.2018 Profile 8	Start: 11:30 End: 13:45 Duration: 2h 15min Waypoints: 15	- 150 m offsets between waypoints. - 143 m between the last two waypoints (WP14 and WP15).
10.10.2018 Profile 9	Start: 11:30 End: 14:25 Duration: 2h 55min Waypoints: 13	- Troubles with tension on the winch at 14:25, survey stopped. - 200 m offsets between waypoints.

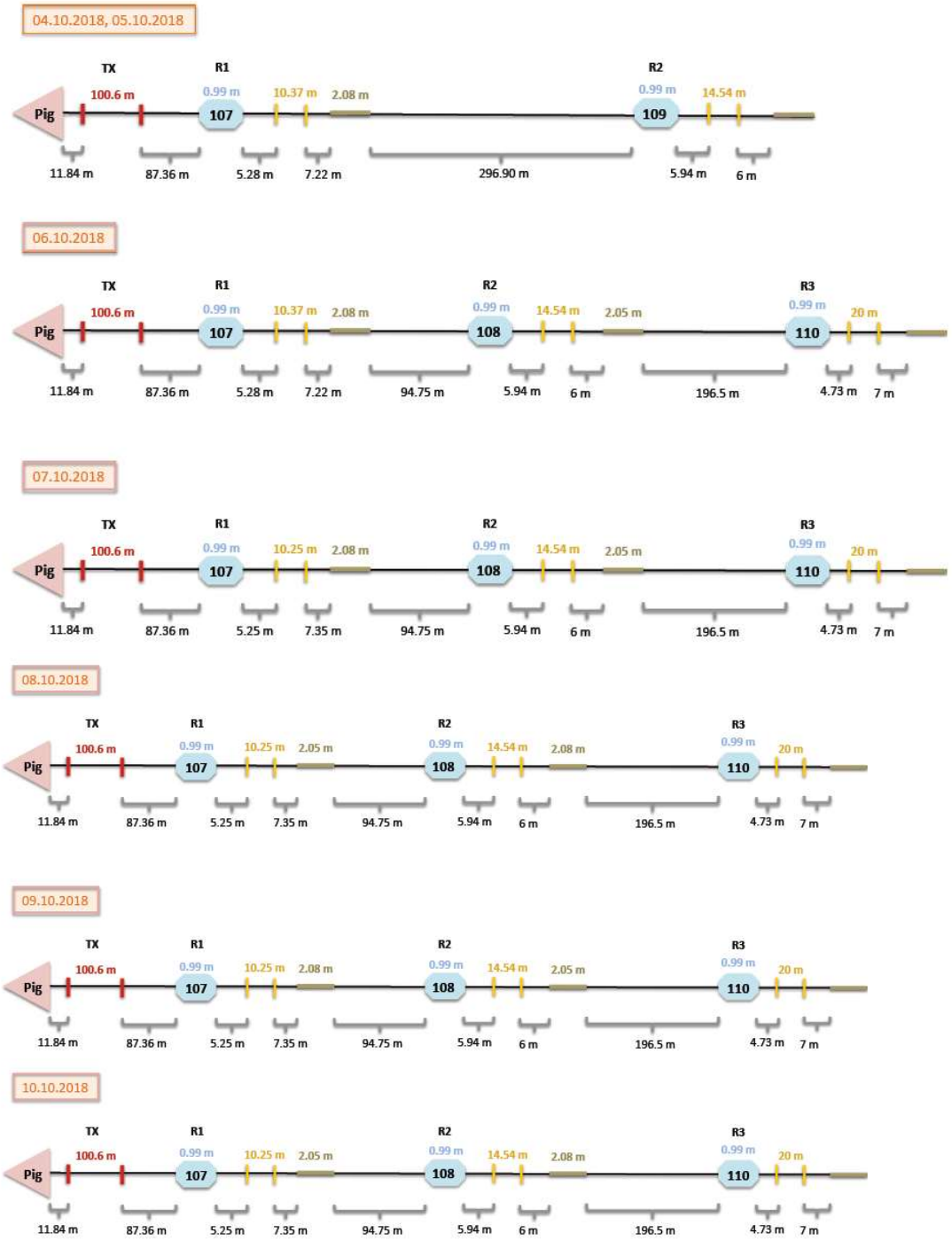

Figure 12: *Geometric settings for each deployment.*

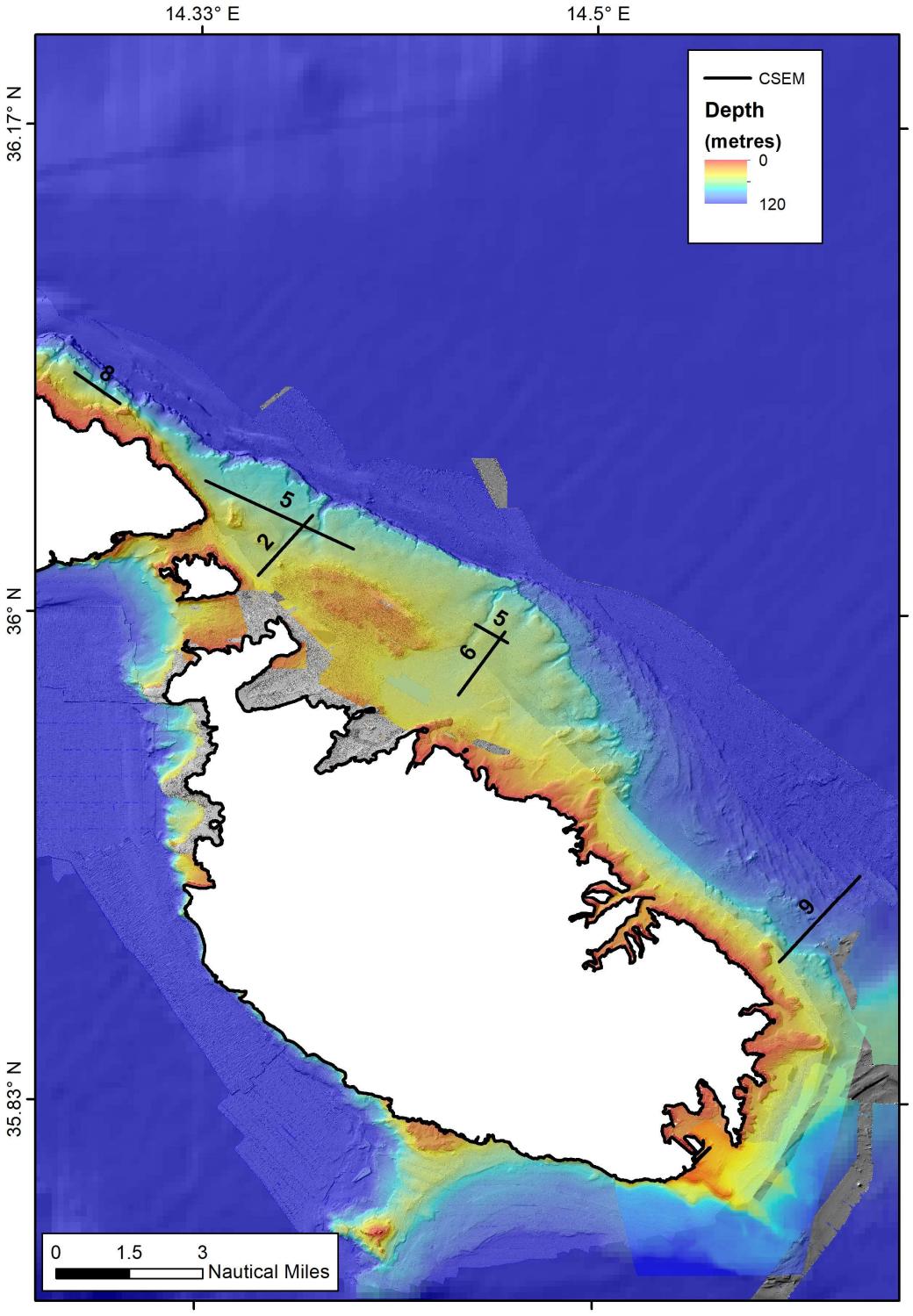

Figure 13: *Location of acquired CSEM transects.*

4.1.4 Data processing

Data processing was carried out using in-house software at GEOMAR that synchronises the measured time series with the source signal. The software subsequently filters, levels and selectively stacks the step-off current functions at each waypoint and for each receiver to optimize data quality before doing the inversion. A step-by-step processing procedure is described below.

1- *Create "Shot Tables" for transmitter raw data.*

Received responses need to be aligned to the exact points in time when the transmitter (TX) current is switched on or off. Thus, the times of switching are identified manually in the transmitter current wave form (red points in Figure 14) and stored in "Shot Table" files.

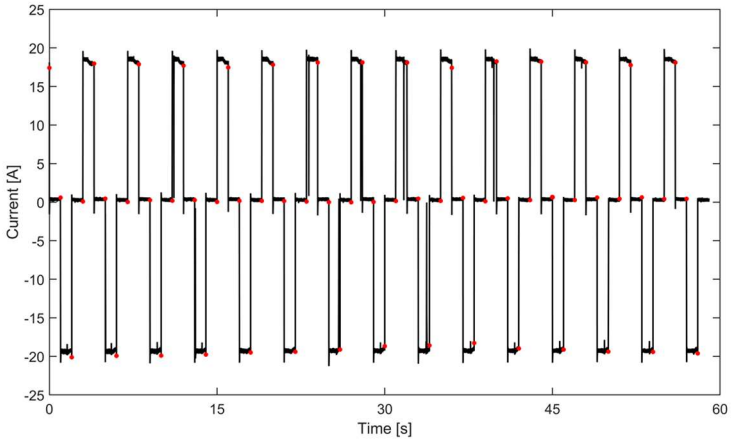

Figure 14: A Shot Table example. "Shot Points" are marked by red dots indicating the time at which the polarity of the signal is changed.

2- *Check clock offsets, synchronization between TX and RXs and correct the drift.*

Time drift between transmitter (TX) and receivers (RXs) are removed by shifting the TX and/or RXs signals forward or backward.

3- *Include the CTD and navigation information in the raw data.*

Shipboard navigation data consist of positions (latitude and longitude) of transmitter and receivers for each measurement point. Conductivity, temperature, and depth of seawater are extracted from CTD data. All the information is combined with CSEM data for each waypoint in a MATLAB structure.

4- *Stack consecutive transients for step-off transmitter waveforms.*

Each signal in one period is divided in four different sub-periods related to the direction of the current switching; zero to positive, positive to zero, zero to negative, and negative to zero. Positive to zero and the negative received values of the negative to zero signals are stacked together to make step-off transients.

In the Malta experiment, CSEM measurements have been done continuously, meaning that data were recorded even when the ship is moving between two consecutive waypoints. Thus, for each waypoint there are a different number of sending files which contain the recorded

60 s signal with the period of 4 s. Among them, two or three sending files belong to the time at which the ship was actually stopped during the measurement. Thus, there are 15, 30, or 45 step-off/on transients at each waypoint, depending on the number of sending files. Transients and standard deviations are calculated using “log-gating” and “gate-stacking” methods as explained by Haroon, 2016.

1D Inversion

The CSEM data were interpreted using a 1D Occam inversion based on “marine transient electromagnetic inversion” (MARTIN) program by Scholl (2010). We assume a 1D layered Earth with certain resistivity and thicknesses of each layer which are changed in the inversion process to reach the minimum misfit of fitting final model to the measured data. There are two main approaches to conduct the inversion. Marquardt inversion relies on the starting model, which we have to define based on the information about the study area, while Occam inversion assumes a model with numerous layers without presumptions. It is usually recommended to do the Occam inversion first and choose afterwards, according to the Occam inversion results, the starting model parameters for the Marquardt inversion. We can then use the best fitting Marquardt inversion model to calculate equivalent models and conduct SVD analysis to estimate resolution of the model parameters.

After establishing that the Occam inversion is able to recover physically reasonable models, we apply the inversion to all stacked step-off transients obtained from processing raw data at each waypoint. We use an Earth model divided into 31 layers with fixed thicknesses as a starting model. Therefore, the model is independent of layer thickness and only depends on the resistivity values of different layers. In order to perform the inversion, we used data between 10^{-3} s to 1 s. For each station, the seawater model (resistivity and water depth) at each waypoint is set to CTD values.

To prevent using unrealistically small amplitudes in early/late times, we started running an Occam inversion setting a minimum relative error to 1%. The inversion results at some stations show a very limited variations in the resistivity as a function of depth while there is not enough resolution to pronounce the existing variation. This seems to be related to the small relative error of measured data which influences the resolution. Therefore, to decrease the minimum value of allowed relative error in 1D inversion results in a higher resolution in the final resistivity model. To improve the resolution of data, we decrease the error model to 0.5% to avoid the domination of short offset influences. Accordingly, 1D inversion for all waypoints were carried out using minimum relative error of 0.5%.

4.2 Seismic reflection profiling

4.2.1 Data Acquisition

Seismic profiling was carried out with a Geo-eel multi-channel high-resolution 2D seismic system. As a source we used a single mini-GI gun with two chambers of 30 cubic inch each. The gun was operated with two diving compressors at 120 - 130 bar. The resulting data were recorded with a Geometrics Geoeel solid state streamer (Figure 15). The streamer consisted of four sections. Each section is 12.5 m long and has eight hydrophone groups yielding seismic 32 channels. Seismic navigation was

based on a dedicated GPS antenna mounted on the bridge deck. The survey setup is depicted in Figure 16. The associated noise level was 150 uPa m at 45 Hz.

Figure 15: *The seismic reflection profiling setup laid out on deck. Shown in the photos are the air gun, streamer and compressors.*

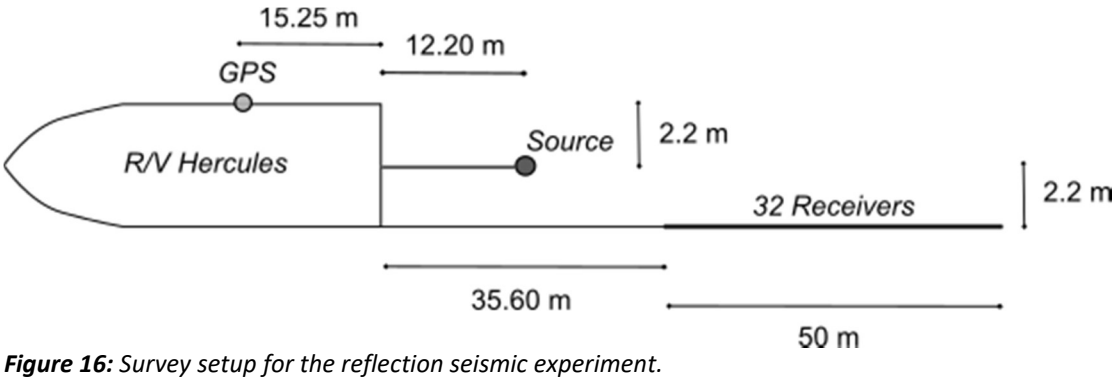

Figure 16: *Survey setup for the reflection seismic experiment.*

We towed the streamer at 4 knots and shot every 5 seconds. Thus, the shot interval was about 10 m depending on currents. During the two days of operations we covered most of the northern shelf of Malta. While surveying on the first day was conducted in fair weather, the sea state deteriorated on the second day and we had to seek shelter for about three hours from 1200-1500. This also resulted in bad data quality for day 2.

On board quality control consisted of plotting of the shot gathers, filtered single channel displays for channel 2 as well as observation of the shot times, frequency and spectra, and noise plots using the Geometrics seismic recording software. A filtered and brute-stacked section of line 3 is shown in Figure 17.

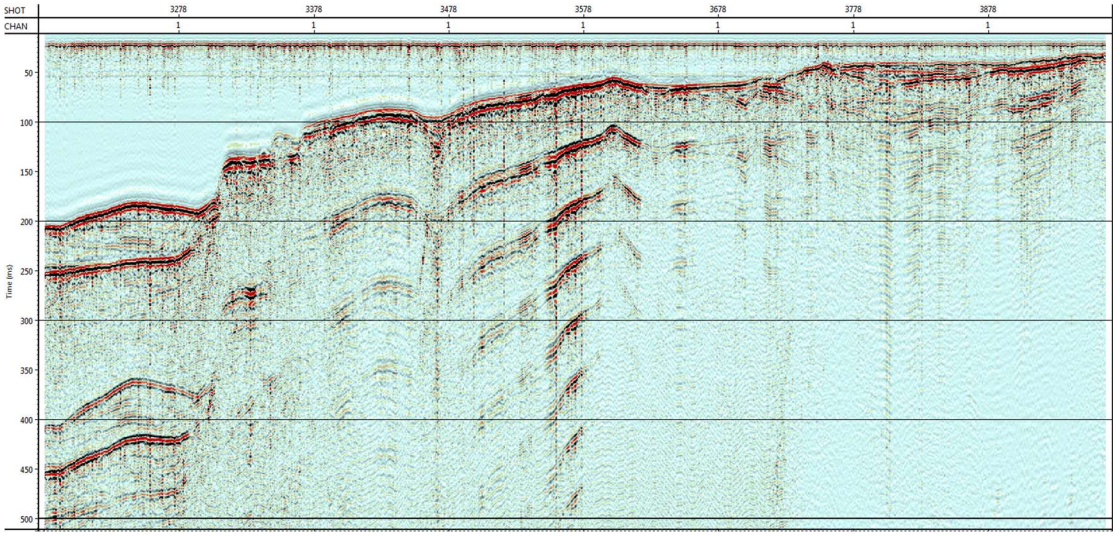

***Figure 17**: Filtered brute stack of Line 3 showing gradual shoaling to the right (S). Up to seven sea floor multiples can be identified in the central part of the line. In the NE off the shelf break seafloor sedimentation is controlled by contour currents.*

Figure 18 shows the spatial coverage of the seismic reflection survey.

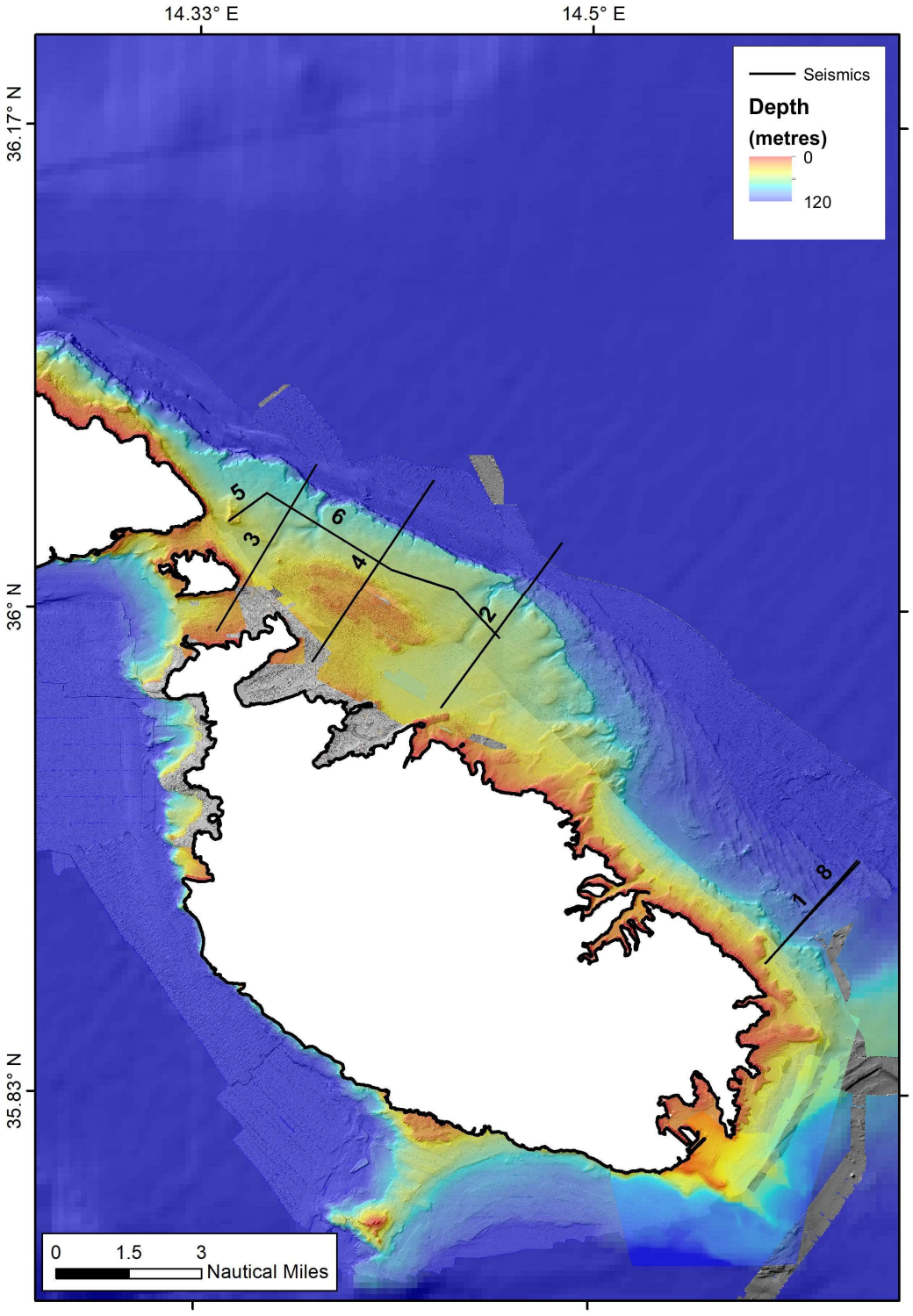

Figure 18: *Location of acquired seismic reflection profiles.*

4.2.2 Data processing

The seismic processing included the streamer geometry configuration using Unix/Fortan scripts developed at *Geomar – Helmholtz Centre for Ocean Research Kiel*. Delay calculations and source and receiver depth control as well as further processing steps were carried out using the Linux-based Seismic Unix processing package. From the seismic data a delay of -27 ms was evaluated for profiles P1000 – P3000 and -35 ms for the profiles P4000 – P8000. A receiver ghost effect in the seismic data could not be detected. The source-receiver locations were binned with a common-midpoint bin spacing of 1.5625 m. Different filter tests were performed and the frequency spectra were analyzed. Seismic traces were balanced and filtered using a bandpass filter with corner frequencies at 30, 50, 420, 500 Hz (P1000, P4000, P5000, P6000, P8000) and 60, 120, 420, 500 Hz (P2000, P3000). The traces were balanced with a rms normalising window starting at 0.05 s. Subsequently, a normal move out correction (with a constant velocity of 1500.00 m/s) and stacking were applied. The stack was migrated with a 2D Stolt algorithm (1500 m/s constant velocity model).

4.3 Water Sampling

Water samples were obtained with a 5 l Niskin bottle from 14 stations (Table 3; Figures 19 and 20). Immediately after the Niskin bottle returned on deck, a drawtube was pre-rinsed with sample water and attached to the Niskin bottle's spigot. Glass and PET flasks were then filled and overflowed, avoiding the formation of air bubbles in order to prevent air contamination. In the PET flasks, a headspace was created and one drop of saturated HCl was added to the sample. All the flasks were stored in the dark.

Geochemical analysis were performed in the laboratories of the Istituto Nazionale di Geofisica e Volcanologia (sezione di Palermo). The chemical composition and concentration of the gases dissolved in seawater samples were determined by using the method in Capasso and Inguaggiato (1998). For the gas chromatography analyses, the sample was split in two aliquots. The first was analysed for O_2, N_2, CH_4 and CO with an Agilent 7890B with two columns in series (Poraplot U 25m×0.53mm and Molsieve 5A 25m×0.53 mm) fluxed by Ar (detectors TDC and FID with methaniser). The second aliquot was analysed for CO_2 by a microGC module (MicroGC 3000) equipped with Poraplot U column (15 m) fluxed by He (detector TCD). Calibration was made with certified gas mixtures. Analytical precision was always better than±3%. The detection limit was ~0.3 ppm for CO and CH_4, 30 ppm for CO_2, and 200 ppm for O_2 and N_2. The isotopic ratio of oxygen ($\delta^{18}O$) was measured using a mass spectrometer Thermo Delta V Plus coupled to a GasBench II that exploits the principle of the head space. For the determination of hydrogen isotopic ratio (δD), we utilised a mass spectrometer Delta Plus XP coupled with a TC/EA reactor. The analytical precision is better than ±0.1% and ±1% for $\delta^{18}O$ and δD, respectively. Isotope ratios are expressed using delta notation as relative differences in parts per mil (δ values %) from Standard Mean Ocean Water (SMOW). The results are shown in Table 4.

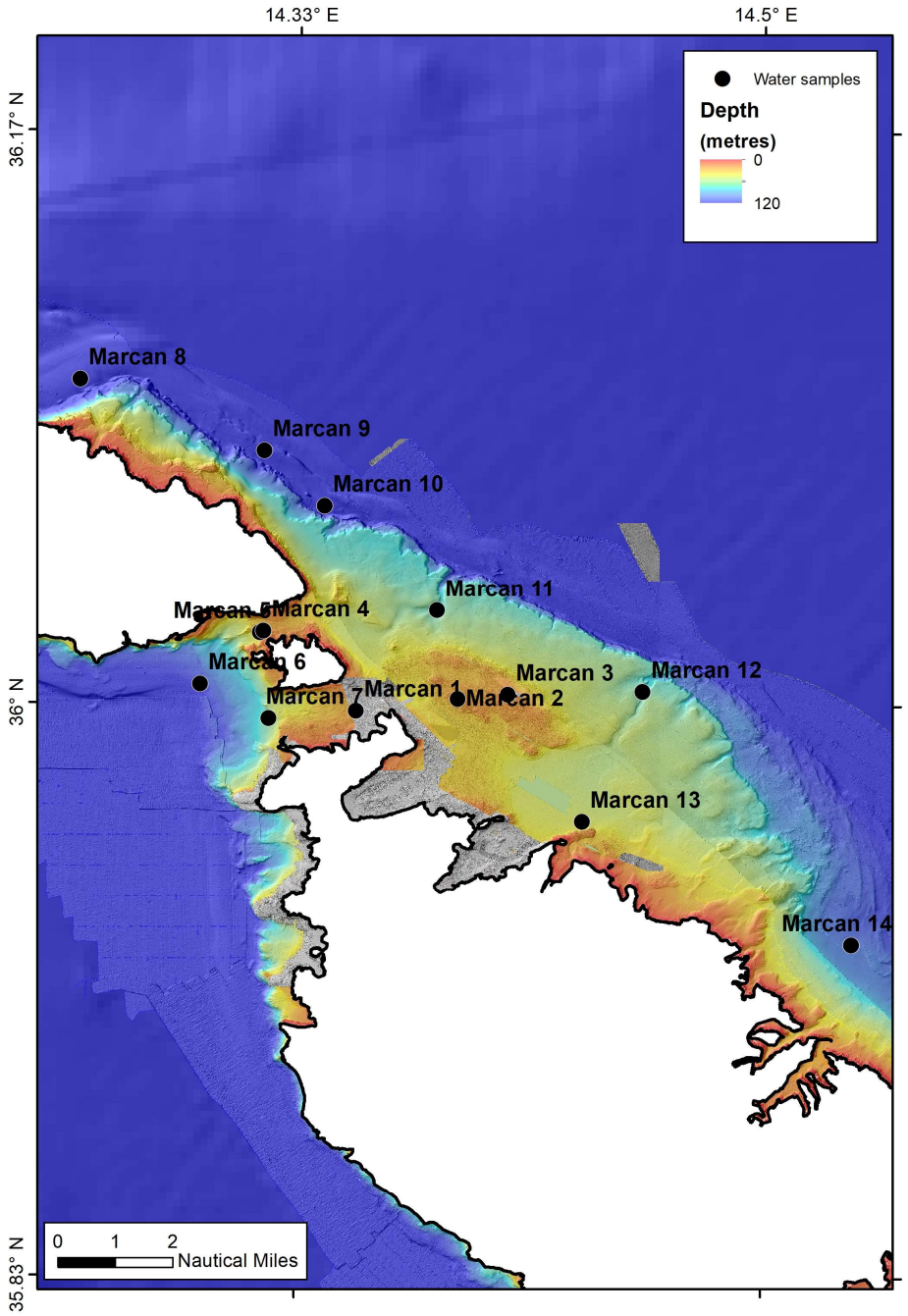

Figure 19: *Location of water samples.*

Figure 20: *Water collection from Niskin bottle.*

Table 3: *Water sample, location and storage strategy.*

Water sample	Date	Time (UTC)	Longitude (°E)	Latitude (°N)	Depth (m)	Glass bottle (250 ml)	Glass bottle (150 ml)	PET bottle (50 ml)	PET bottle (50 ml) + HCl
1	7.10	08:00	14.354285	35.998299	22		X	X	
2	8.10	06:30	14.390734	36.001649	18	X	X	X	X
3	8.10	06:45	14.40866	36.003001	14	X	X	X	X
4	8.10	15:00	14.320966	36.021182	24			X	X
5	8.10	15:15	14.319832	36.020714	31	X	X	X	X
6	8.10	15:30	14.2985	36.0057	108	X	X	X	X
7	8.10	15:45	14.323093	35.995809	67	X	X	X	X
8	9.10	07:30	14.254796	36.094138	150	X	X	X	X
9	9.10	13:10	14.320993	36.073774	130	X	X	X	X
10	9.10	13:30	14.342722	36.057778	130	X	X	X	X
11	9.10	14:50	14.383111	36.027562	74	X	X	X	X
12	9.10	15:20	14.457029	36.004041	79	X	X	X	X
13	9.10	15:55	14.435578	35.966172	47	X	X	X	X
14	9.10	16:30	14.532124	35.930413	103	X	X	X	X

***Table 4**: Geochemical results.*

Sample	δD	$\delta^{18}O$	O_2 ccSTP	N_2 ccSTP	CO ccSTP	CH_4 ccSTP	CO_2 ccSTP
Marcan 2	6.22	1.16	0,15	9,61	7,30E-05	1,09E-03	1,02
Marcan 3	6.88	1.01	0,96	8,89	0,00E+00	2,10E-04	0,58
Marcan 5	8.96	1.23	0,12	9,00	0,00E+00	1,29E-03	0,50
Marcan 6	6.35	0.92	0,30	0,91	0,00E+00	0,00E+00	0,03
Marcan 7	7.34	1.09	4,00	9,68	8,06E-04	2,35E-04	0,44
Marcan 8	7.69	1.21	3,29	8,10	0,00E+00	1,61E-03	0,56
Marcan 9	8.52	1.14	1,99	9,83	0,00E+00	9,36E-04	0,66
Marcan 10	6.80	1.24	1,02	9,67	0,00E+00	8,34E-04	0,70
Marcan 11	7.33	0.92	0,34	9,76	4,95E-04	1,42E-03	1,14
Marcan 12	8.01	0.99	1,56	10,60	0,00E+00	1,63E-03	0,54
Marcan 13	7.83	1.18	0,28	8,51	6,11E-05	2,11E-03	0,81
Marcan 14	9.22	1.32	0,21	9,15	0,00E+00	1,84E-03	0,59

5. Narrative of Cruise

All times in UTC

Monday, October 1
Manoel Island-Cirkewwa
The vessel departed Manoel Island at 06:00. However, due to a problem with the compressor and a missing part, we had to head back to Manoel Island and departed again at 9:00. The workstation developed a software issue, and we could only start data acquisition at 10:30. We completed data acquisition at 15:30, after which we headed to Cirkewwa.

Tuesday, October 2
Cirkewwa-Manoel Island
Due to a problem with the compressor fuel, departure from Cirkewwa took place at 06:20. There was a problem with the A-frame, which was soon solved and data acquisition started at 07:12. The vessel encountered bad weather, especially between 08:25 and 10:45. Data acquisition was completed at 15:40, after which we headed to Manoel Island.

Wednesday, October 3
Manoel Island-Manoel Island
Mobilisation of the CSEM equipment started at 11:00 after the seismic gear was offloaded from the RV Hercules. Labs were set up and the transmitter and receiver dipoles were set up on deck. Due to the fact that an ROV head was installed underneath the main block of the A-frame, which could not be dismantled, we attached our block starboard from the ROV head on the A-frame. At 15:30 we performed a successful test deployment just outside the harbour of the depressor containing the transmitter (Pig) via the crane through the A-frame.

Thursday, October 4
Manoel Island - Manoel Island
The first action of the day was to try to feed the Konsgberg transponder navigation data into OFOP. However, this could not be achieved since the shipboard system was not set up to supply NMEA strings needed by OFOP. We therefore decided to plan our profiles via ArcGIS and monitor online the position of the transponder using the Fledermaus software installed on the vessel, which could read and display the Kongsberg strings. The positions received by Fledermaus were logged.
At 10:35 we moved to 1 nm before the eastern starting point of the coast-perpendicular line 9 and performed another test deployment of the Pig, this time with the CTD. While checking the receiver dipoles on deck before deployment, damage was observed on two of the electrical dipoles, such that we decided to deploy two receivers only and to start the construction of two new dipoles from spare parts.
At 12:00 we deployed the two receivers and Pig. Before waypoints could be obtained, transmitter synchronisation failed. To acquire some test data we occupied three test way points and recovered the streamer. Recovery of the instrumentation was initiated after 16:00 and completed at 18:00. Since it was hard manual work to pull in the streamer over the stern directly, we decided to install a block under the ROV head in the A-frame to facilitate and speed up deployment and recovery of receiver string.
The synchronisation of the transmitter was probably lost due to the fact that the pressure cylinder containing the buffering batteries moved within the pig during deployment. Subsequently, we secured the battery pack with belts and the problem did not occur again

afterwards. Furthermore, the TX connectors were damaged due to the battery pack movement.

Friday, October 5
Manoel Island-Manoel Island
The day started with the repair of the transmitter connectors, after which we headed out to profile 9 again. We deployed a system with two receivers between 11:10 and 12:40. Ten waypoints were acquired until 15:40, when connection to transmitter was lost. The reason for this was a data communication problem from the transmitter of unknown origin. As a precaution, the controlling transmitter software was reinstalled and the problem did not occur again. While data communication was lost in between, there was no problem with the time keeping on the transmitter and the system could be synchronized once on deck.

Saturday, October 6
Manoel Island - Cirkewwa
Originally we planned to occupy profile 5 on this day. However, while discussing navigation on the bridge we became aware of a fish farm in the centre of the profile, which had to be avoided. We decided therefore to occupy profile 6 instead, on which we started data acquisition at 09:26 with 3 receivers and acquired 11 way points. To acquire some data points along the southern end of profile 5 we decided to not recover and deploy the system (estimated time 3 hours), but initiated a turn of the entire array on the seafloor (12:30 to 15:00) to head into profile 5. The transmitter transmission was shut down between 12:30 and 13:20, since the array was not aligned during this time and thus TX-RX geometry not sufficiently well known to have meaningful data. On profile 5 we acquired 4 waypoints crossing a palaeo channel. Data acquisition had to be stopped at 16:00 to head into port at a reasonable time, since we booked a lot of overtime on previous days. Unfortunately, the electrode cable of R1 was broken and R3 had lost time at after way point 11. The damage to both receivers were probably caused by obstacles on the seafloor, or strains on the array during the turn.

Sunday, October 7
Cirkewwa-Cirkewwa
The land-perpendicular profile 2 in the northern segment was occupied during this day. Data acquisition with three receivers started at 11:09 and we successfully acquired 16 waypoints along the profile. Data acquisition was stopped at 14:00 and the streamer and pig recovered successfully. We also acquired one water sample.

Monday, October 8
Cirkewwa-Cirkewwa
During this day, a film team (Dr. Tamara Worzewski and Kameraman Johannes Zerbst) joined us to document the research on offshore groundwater exploration. We occupied the northern end of the coast parallel profile 5. The first waypoint of 24 waypoints could be occupied at 9:00, and data acquisition proceeded up to 14:00. During the day, various interviews were conducted on the ship with scientists and technicians. After recovery of the streamer, we headed back to port and had an evening BBQ on the ship celebrating the successful data acquisition of the previous days. Six water samples were also acquired.

Tuesday, October 9
Cirkewwa-Manoel Island
We occupied the coast-parallel profile 8 offshore Gozo on this day and successfully acquired 15 waypoints between 9:00 and 12:00. In addition to the three receivers from the BGR, we

also made a first successful test deployment of our newly designed GEOMAR receiver dipole, which was attached to the receiver at the very end behind R3. Since it was not possible to occupy another profile during the remaining time, we returned to Cirkewwa, where the camera team and all scientists besides Prof. Micallef and Dr. Spatola got off the ship. The latter acquired seven water samples along the transit of RV Hercules towards Manoel Island. Dr. Schwalenberg and Dr. Jegen conducted interviews on the pier in Cirkewwa until about 16:30.

Wednesday, October 10
Manoel Island - Manoel Island
We originally planned to occupy the remaining segment of the coast-perpendicular profile 10 during this day. However, it was discovered that the profile ran along a power line leading into Valletta. Since the profile could not be moved north or south due to the possibility of crossing other power lines, getting into the main ship track into the harbour, or hitting seafloor bedrock, we decided to reoccupy profile 9, which could not be fully acquired on October 4th and 5th. Similarly as the day before, we deployed three BGR receiver dipoles as well as the GEOMAR dipole. We successfully acquired 13 way points along the profile between 10:00 and 12:15, when suddenly the tension on the winch cable rose to above 1000 N, indicating that the streamer got stuck on the seafloor. We immediately paid out more winch cable and then proceeded to move the shop astern while at the same time heaving in the cable. After a very tense and nerve-wracking half hour, the streamer got loose during the manoeuvre and could be fully recovered. However, during the obstruction, the tension was so high that the connection of the winch cable with the pig was damaged and the termination needed to be severed when on deck. At the end of the day, we packed all boxes and assembled stacks on the deck.

Thursday, October 11
Dr Jegen, Mr Wollatz-Vogt and Dr Schwalenberg returned to the vessel in the morning to oversee the last preparations for loading the gear into the container and left at 11:00 to head to the airport/workshop at the University of Malta.

6. Acknowledgements

The survey was funded by the European Union's Horizon 2020 Programme (grant agreement n° 677898 (MARCAN)). We kindly acknowledge captain and crew of the R/V Hercules. We thank the Maltese authorities for permissions to carry out the marine surveys.

7. Appendix

Station List CSEM

WayPoint	Station	Duration	Current	1/Frequency	Time	x	y	z	Comment
Profile 9	Oct. 5								
Transit	1000	60	20	2	Start Measurements PIG on the seafloor				
WP001	1001	60	20	2	13:42:00	14.61112	35.91103	125	
Transit	1002	60	20	2	13:47:00				
WP002	1003	60	20	2	13:56:00	14.6091	35.90903	127.11	
Transit	1004	60	20	2	14:00:00				
WP003	1005	60	20	2	14:07:00	14.60457	35.90369	124	
Transit	1006	60	20	2	14:10:00				
WP004	1007	60	20	2	14:19:00	14.60243	35.90484	130	
Transit	1008	60	20	2	14:22:00				
WP005	1009	60	20	2	14:29:00	14.60018	35.90277	133	
Transit	1010	60	20	2	14:32:00				
Wp006	1011	60	20	2	14:40:00	14.60045	35.90082	123	
Transit	1012	60	20	2	14:42:00				
WP007	1013	60	20	2	14:49:00	14.59817	35.89882	130	
Transit	1014	60	20	2	14:52:00				
WP008	1015	60	20	2	14:59:00	14.59566	35.89691	118	
Transit	1016	60	20	2	15:02:00				
WP09	1017	60	20	2	15:10:00	14.59394	35.89507	115	
Transit	1018	60	20	2	15:20:00				17:18 reboot of transmitter
WP10	1018	60	20	2	15:38:00	14.59069	35.89271	??	Eithernet on Laptop broken,
Abort									

Profile 6	**Oct. 6**				Profile 6				
Transit	2000	60	20	2					
WP001	2001	60	20	2	09:44:00	14.46193	35.99359	68	
Transit	2002	60	20	2	09:49:00				
WP002	2003	60	20	2	09:59:00	14.46005	35.99133	66.6	Water depth from bridge 53 m
Trnasit	2004	60	20	2	10:03:00				
WP003	2005	60	20	2	10:10:00	14.45877	35.98985	69	
Transit	2006	60	20	2	10:16:00				
WP004	2007	60	20	2	10:25:00	14.45435	35.98711	90	Water depth from bridge 53 m
Transit	2008	60	20	2	10:33:00				
WP005	2009	60	20	2	10:44:00	14.45486	35.98546	65	Water depth from bridge 52 m
Transit	2010	60	20	2	10:49:00				
WP006	2011	60	20	2	10:59:00	14.45296	35.98324	65	
Transit	2012	60	20	2	11:03:00				
WP007	2013	60	20	2	11:13:00	14.45106	35.98108	61.94	
Transit	2014	60	20	2	11:19:00				
WP08	2015	60	20	2	11:29:00	14.44878	35.9787	59.75	
Transit	2016	60	20	2	11:34:00				
WP09	2017	60	20	2	11:46:00	14.4472	35.97676	55.2	
Transit	2018	60	20	2	11:59:00				
WP10	2019	60	20	2	12:09:00	14.44499	35.9747	60.33	
Transit	2020	60	20	2	12:11:00				
WP11	2021	60	20	2	12:22:00	14.44295	35.97245	60.63	
Profile 5	**Oct. 6**								
WP001	2023	60	20	2	14:57:00	14.46173	35.99066	67.3	Only one send cycle
Transit	2024	60	20	2	15:02:00				
WP002	2025	60	20	2	15:11:00	14.4588	35.99182	65.11	
Transit	2026	60	20	2	15:17:00				
WP003	2027	60	20	2	15:29:00	14.45584	35.99313	63.84	

Transit	2028	60	20	2	15:34:00				
WP004	2029	60	20	2	15:54:00	14.4505	35.99556	69.8	
Profile 2	**Oct. 7**								
Test Measurements	3000	60	20	2		14.35863	36.00737	20.24	
	3001	60	20	2					120 m Cable Length
WP001	3002	60	20	2	10:50:00	14.35865	36.01293	55.68	Water Depth from Bridge 44 m
Transit	3003	60	20	2	10:56:00				
WP002	3004	60	20	2	11:06:00	14.36004	36.01609	136	Water Depth from Bridge 46 m
Transit	3005	60	20	2	11:12:00				
WP003	3006	60	20	2	11:22:00	14.36226	36.01641	55	47 m
Transit	3007	60	20	2	11:30:00				140 m Cable out 11:34
WP004	3008	60	20	2	11:41:00	14.36685	36.01834	53.32	Water Depth from Bridge 49 m
Transit	3009	60	20	2	11:46:00				
WP005	3010	60	20	2	11:58:00	14.3664	36.0204	65	Water Depth from Bridge 53 m
Transit	3011	60	20	2	12:04:00				
WP006	3013	60	20	2	12:10:00	14.37018	36.0217	82	54 m
Transit	3014	60	20	2	12:16:00				
WP007	3015	60	20	2	12:22:00	14.36862	36.02243	62	55 m
Transit	3016	60	20	2	12:26:00				
WP008	3017	60	20	2	12:31:00	14.36971	36.02344	66	59
Transit	3018	60	20	2	12:38:00				
WP009	3019	60	20	2	12:45:00	14.37977	36.02442	77.9	59
Transit	3020	60	20	2	12:53:00				
WP010	3021	60	20	2	12:58:00	14.37464	36.02572	101	63
Transit	3022								
WP011	3023	60	20	2	13:09:00	14.37227	36.02676	77	65 m
Transit	3024	60	20	2	13:14:00				
WP012	3025	60	20	2	13:21:00	14.37487	36.02811	76	63 m
Transit	3026	60	20	2	13:26:00				
WP013	3027	60	20	2	13:33:00	14.37633	36.02945	76	65 m

Transit	3028	60	20	2	13:38:00				
WP014	3029	60	20	2	13:45:00	14.37785	36.03066	88	67 m
Transit	3030	60	20	2	13:54:00				
WP015	3031	60	20	2	14:01:00	14.38073	36.03488	85	69 m
Transit	3032	60	20	2	14:06:00				
WP016	3033	60	20	2	14:13:00	14.38077	36.03319	83	70 m
Profile 5	**Oct. 8**								
Test Measurements	4000	60	20	2	08:36:00	14.40103	36.02093	33	Measurement in the water column
		60	20	2					
WP001	4001	60	20	2	08:56:00	14.39802	36.0222	63.7	59 m from Bridge
Transit	4002	60	20	2	09:02:00				300 m transfer
WP002	4003	60	20	2	09:21:00	14.395	36.02311	75	58 m
Transit	4004	60	20	2	09:25:00				300 m transfer
WP003	4005	60	20	2	09:34:00	14.39197	36.02417	75	61 m
Transit	4006	60	20	2	09:39:00				300 m transfer
WP004	4007	60	20	2	09:51:05	14.3889	36.02526		62 m
Transit	4008	60	20	2	09:56:00				300 m trsfer
WP005	4009	60	20	2	10:05:00	14.38246	36.02683		71 m
Transit	4010	60	20	2	10:10:00				300 m transfer
WP006	4011	60	20	2	10:19:00	14.38278	36.02757		67 m
Transit	4012	60	20	2	10:24:00				100 m transfer
WP007	4013	60	20	2	10:28:00	14.38179	36.02793		54 m
Transit	4014	60	20	2	10:32:00				150 m transfer
WP008	4015	60	20	2	10:37:00	14.3803	36.02842		63 m
Transit	4016	60	20	2	10:41:00				150 m transfer
WP009	4017	60	20	2	10:46:35	14.38878	36.02905		63 m
Transit	4018	60	20	2	10:51:00				150 m transfer
WP010	4020	60	20	2	10:55:15	14.37729	36.02958		65 m
Transit	4021	60	20	2	10:59:15				150 m transfer
WP011	4022	60	20	2	11:04:20	14.37579	36.03018		65 m

Transit	4023	60	20	2	11:09:00				300 m transfer
WP012	4024	60	20	2	11:18:00	14.37279	36.03137		66 m
Transit	4025	60	20	2	11:22:00				300 m transfer
WP013	4026	60	20	2	11:33:19	14.36978	36.03258		63 m
Transit	4027	60	20	2	11:38:00				300 m transfer
WP014	4028	60	20	2	11:49:00	14.36534	36.03628		62 m
Transit	4029	60	20	2	11:55:00				300 m transfer
WP015	4030	60	20	2	12:05:45	14.36378	36.03489		62 m
Transit	4031	60	20	2	12:11:00				300 m transfer
WP016	4032	60	20	2	12:18:53	14.35757	36.03684		65 m
Transit	4033	60	20	2	12:23:00				300 m transfer
WP017	4036	60	20	2	12:30:00	14.35774	36.03716		65 m
Transit	4037	60	20	2	12:35:00				300 m transfer
WP018	4038	60	20	2	12:42:20	14.35156	36.03838		67 m
Transit	4039	60	20	2	12:47:00				300 m transfer
WP019	4040	60	20	2	12:56:02	14.35166	36.03937		68 m
Transit	4041	60	20	2	13:00:00				300 m transfer
WP020	4042	60	20	2	13:07:11	14.34862	36.04041		69 m
Transit	4043	60	20	2	13:12:00				300 m transfer
WP021	4044	60	20	2	13:18:45	14.34555	36.04156		69 m
Transit	4045	60	20	2	13:22:00				300 m transfer
WP022	4046	60	20	2	13:30:10	14.35257	36.40427		68 m
Transit	4047	60	20	2	13:34:00				300 m transfer
WP023	4048	60	20	2	13:42:10	14.33951	36.04382		65 m
Transit	4049	60	20	2	13:46:00				300 m transfer
WP024	4050	60	20	2	13:53:00	14.33652	36.04491		59 m
Profile 8	**Oct. 9**								
Test Measurements	5000	60	20	2					
		60	20	2					
WP001	5001	60	20	2	09:36:00	14.27996	36.08153	69	58 m water depth

Transit	5002	60	20	2	09:41:00				150 m transfer
WP002	5003	60	20	2	09:45:00	14.28137	36.08082		61 m
Transit	5004	60	20	2	09:49:00				150 m transfer
WP003	5005	60	20	2	09:52:00	14.28278	36.08006		62 m
Transit	5006	60	20	2	09:56:00				150 m transfer
WP004	5007	60	20	2	10:03:00	14.28353	36.07714		
Transit	5008	60	20	2	10:08:00				150 m transfer
WP005	5009	60	20	2	10:11:00	14.28828	36.07821		
Transit	5010	60	20	2	10:15:00				150 m transfer
WP006	5011	60	20	2	10:24:00	14.28699	36.07781		
Transit	5012	60	20	2	10:28:00				150 m transfer
WP007	5013	60	20	2	10:34:00	14.28837	36.07711		
Transit	5014	60	20	2	10:38:00				150 m transfer
WP008	5015	60	20	2	10:42:00	14.28983	36.07641		
Transit	5016	60	20	2	10:46:00				150 m transfer
WP009	5017	60	20	2	10:52:00	14.29124	36.07565		
Transit	5018	60	20	2	10:56:00				150 m transfer
WP010	5019	60	20	2	11:01:00	14.29263	36.07513		
Transit	5020	60	20	2	11:04:00				150 m transfer
WP011	5021	60	20	2	11:08:00	14.29401	36.0742		
Transit	5022	60	20	2	11:12:00				150 m transfer
WP012	5023	60	20	2	11:16:00	14.29545	36.07319		
Transit	5024	60	20	2	11:20:00				150 m transfer
WP013	5025	60	20	2	11:24:00	14.29683	36.07282		
Transit	5026	60	20	2	11:27:00				150 m transfer
WP014	5027	60	20	2	11:32:00	14.29822	36.07207		
Transit	5028	60	20	2	11:36:00				143 m transfer
WP015	5029	60	20	2	11:00:00	14.29956	36.0714		
Profile 9	**Oct. 10**								Comment
Test Measurements	6000	60	20	2					

		60	20	2					
WP001	6001	60	20	2	09:52:00	14.59638	35.89658	105	
Transit	6002	60	20	2	09:58:00				200 m Transit
WP002	6003	60	20	2	10:05:50	14.59513	35.89521	102	
Transit	6004	60	20	2	10:10:00				200 m Transit
WP003	6005	60	20	2	10:17:24	14.59559	35.89712	105	
Transit	6006	60	20	2	10:22:00				200 m Transit
WP004	6007	60	20	2	10:27:49	14.59417	35.89536	103	
Transit	6008	60	20	2	10:32:00				200 m Transit
WP005	6009	60	20	2	10:37:34	14.59271	35.89445	99	
Transit	6010	60	20	2	10:43:00				200 m Transit
WP006	6011	60	20	2	10:48:34	14.59123	35.89311	98	
Transit	6012	60	20	2	10:54:00				200 m Transit
WP007	6013	60	20	2	11:00:00	14.5897	35.88853	95	
Transit	6014	60	20	2	11:06:00				200 m Transit
WP008	6015	60	20	2	11:11:00	14.58373	35.89014	92	
Transit	6016	60	20	2	11:16:00				200 m Transit
WP009	6017	60	20	2	11:21:38	14.5868	35.88911	86	
Transit	6018	60	20	2	11:26:00				200 m Transit
WP010	6019	60	20	2	11:31:00	14.58537	35.88774	78	
Transit	6020	60	20	2	11:36:00				200 m Transit
WP011	6021	60	20	2	11:42:00	14.58391	35.88643	72	
Transit	6022	60	20	2	11:46:00				200 m Transit
WP012	6023	60	20	2	11:51:35	14.57809	35.8819	61	
Transit	6024	60	20	2	11:56:00				200 m Transit
WP013	6025	60	20	2	12:01:00	14.57679	35.88409	54	
Transit	6026	60	20	2	12:12:00				200 m Transit
WP014	6027	60	20	2					
Transit	6028	60	20	2					
WP015	6029	60	20	2					

Station List Seismics

Date	Time	File name	Line	Latitude (°N)	Longitude (°E)	Speed (kn)	Heading (°)	Depth	Pressure (bar)	Remarks
01.10	10:27		1	35°52.6839	14°34.4794	4.6	35	39.4		SOL 1 – compressor refuelled
	10:35	380		35°52.9462	14°34.7699	4.5	35	55.1	90	Continuing
	11:11	810		35°54.8171	14°36.8668	4.3	35	113.2		EOL 1
	12:35	2115	2	36°01.4046	14°29.2705	4.3	205	133.8		SOL2
		2226								Error
	12:49	2236		36°00.6000	14°28.5820	4.3	226	108.0		Back on track
	13:35	2857		35°57.9585	14°26.1700	4.4	227	43.4		EOL 2
	14:33	3179	3	36°02.9823	14°23.0000	4.7	235	147.0		SOL 3
	14:35	3965		35°59.4917	14°20.4742	4.3	237	14.5		EOL 3
02.10	06:58	4001								
	07:11	4174	4	35°58.8918	14°22.9009	4.3	26	30.5	80	SOL 4
	08:14	4957		36°02.6873	14°25.9997	4.3	38	146.5		EOL 4
	10:44	5000	5	36°01.8120	14°20.7816	3.6	59	29.8		SOL 5
	10:57	5161		36°02.3982	14°21.7389	4.4		68.9		EOL 5
	11:05	6000	6	36°02.3756	14°21.7365	4.4	119	67.9		SOL 6
	11:46	6536		36°00.8294	14°24.9156	4.3	109	50.2		Course altered to avoid running into fish farm
	12:08	6784		36°00.4320	14°26.4550	4.5	123	51.2		Continue line 6
	12:25	6992		35°59.4200	14°27.6794	4.3	113	54.4		EOL 6
										Transit

	15:01	9246	8	35°54.8357	14°36.8064	4.4	226	112.2		SOL 8
	15:41	9738		35°52.6901	14°34.4507	4.5	222	36.9		EOL8

References:

Capasso, G., Inguaggiato, S., 1998. A simple method for the determination of dissolved gases in natural waters. An application to thermal waters from Vulcano Island. Appl.

Geochem. 13 (5), 631–642. https://doi.org/10.1016/S0883-2927(97)00109-1.Haroon, Amir, 2016. Development of novel time-domain electromagnetic methods for offshore groundwater studies: A data application from Bat Yam, Israel. Diss. Universität zu Köln.

Micallef, A., Spatola, D., Caracausi, A., Italiano, F., Barreca, G., D'Amico, S., Petronio, L.R.M., Coren, F., Facchin, L., Blanos, R., Pavan, A., Paganini, P., Taviani, M., 2019. Active degassing across the Maltese Islands (Mediterranean Sea) and implications for its neotectonics. Marine and Petroleum Geology, 104, 361-374.

Scholl, C., 2010. Resolving an Onshore Gas-hydrate Layer with Long-offset Transient Electromagnetics (LOTEM). In: M. Riedel, E. C. Willoughby & C. Chopra, eds. Geophysical Characterization of Gas Hydrates. s.l.:Society of Exploration Geophysicists, pp. 149-162.